Princeton Plasma Physics Laboratory

PPPL- 4414

PPPL- 4414

Theory of Fine-scale Zonal Flow Generation From Trapped Electron Mode Turbulence

L. Wang and T.S. Hahm

June, 2009

Prepared for the U.S. Department of Energy under Contract DE-AC02-09CH11466.

Theory of fine-scale zonal flow generation from trapped electron mode turbulence

Lu Wang[1,2] and T.S. Hahm[2]
[1]School of Physics, Peking University, Beijing 100871, China
[2]Princeton University, Princeton Plasma Physics Laboratory
P. O. Box 451, Princeton, NJ 08543, USA

(Dated: June 2, 2009)

Abstract

Most existing zonal flow generation theory has been developed with a usual assumption of $q_r\rho_{\theta i} \ll 1$ (q_r is the radial wave number of zonal flow, and $\rho_{\theta i}$ is the ion poloidal gyroradius). However, recent nonlinear gyrokinetic simulations of trapped electron mode (TEM) turbulence exhibit a relatively short radial scale of the zonal flows with $q_r\rho_{\theta i} \sim 1$ [Z. Lin et al., IAEA-CN/TH/P2-8 (2006); D. Ernst et al., Phys. Plasmas **16**, 055906 (2009)]. This work reports an extension of zonal flow growth calculation to this short wavelength regime via the wave kinetics approach. A generalized expression for the polarization shielding for arbitrary radial wavelength [Lu Wang and T.S. Hahm, to appear in Phys. Plasmas (2009)] which extends the Rosenbluth-Hinton formula in the long wavelength limit is applied.

I. INTRODUCTION

An important role of zonal flows (ZF) in regulating turbulence and transport is now broadly accepted.[1,2] Most gyrokinetic simulation studies highlighting the crucial role of ZFs concentrated on ion temperature gradient (ITG) turbulence.[3,4] Since anomalous electron heat transport is ubiquitously observed from experiments even when the ITG mode seems stable, it's important to study ZF driven by trapped electron modes (TEMs). The collisionless TEM (CTEM) is driven by the trapped electron precession drift resonance,[5] and is considered to be an important potential contributor to the electron anomalous transport in the core of fusion devices. Theoretical calculations of the nonlinearity associated with magnetically trapped electrons have been extensively investigated previously.[6–12] The TEM driven turbulence and transport have also been studied experimentally in some tokamaks, such as ASDEX upgrade,[13] Alcator C-Mod,[14] and DIII-D.[15]

Recently, some gyrokinetic simulation works have paid more attention to ZF effects on the CTEM turbulence.[14,16–21] The nonlinear upshift of the critical density gradient for CTEMs due to suppression by turbulence-generated ZFs was reported,[14] which is analogous to the case for ITG modes.[4] On the other hand, weak influence of ZFs on the transport level was claimed for different parameter regimes.[16] These different behaviors are not necessarily in conflict due to parametric dependencies.[18,19] The geodesic acoustic modes' contribution to the shearing effects of ZFs is found to be insignificant in Ref. 20, which is consistent with previous predictions.[22]

So far, there are very few theoretical works[23] on ZFs in CTEM turbulence driven by the trapped electron precession drift resonance. In most existing ZF generation theories,[24,25] the Rosenbluth-Hinton (R-H) formula[26] for neoclassical polarizability $1.6\epsilon^{3/2}q_r^2\rho_{\theta i}^2$ was used, where ϵ is the inverse aspect ration, q_r is the radial wave number of the ZF, $\rho_{\theta i} = (T_i/m_i)^{1/2}/\Omega_p$ is the ion poloidal gyroradius, and $\Omega_p = eB_\theta/(m_i c)$ is the ion poloidal gyrofrequency. This formula is valid only for the long wavelength limit, i.e., $q_r\rho_{\theta i} \ll 1$. However, relatively short scale ZFs, i.e., $q_r\rho_{\theta i} \sim 1$, have been found in recent nonlinear gyrokinetic simulations of CTEM turbulence.[17,20,21] The goal of this work is hence to extend the ZF growth calculation to this short wavelength regime.

In the present work, we analytically study the ZF generation in CTEM turbulence. We adopt the simple theoretical model of the dispersion relation and the linear growth rate for the CTEM in Ref. 5. We also investigate the variation of the ZF growth rate normalized to the CTEM intensity in gyro-Bohm units with plasma parameters, including the normalized density gradient R/L_n, where $L_n^{-1} = -\partial \ln n_0/\partial r$, normalized electron temperature gradient R/L_{T_e}, where $L_{T_e}^{-1} = -\partial \ln T_e/\partial r$, electron to ion temperature ratio $\tau = T_e/T_i$, and the wavelength of the ambient CTEM turbulence $k_\perp\rho_i$, where $k_\perp$ refers to the perpendicular component of CTEM wave vector, $\rho_i = (T_i/m_i)^{1/2}/\Omega_i$ is the ion gyroradius, and $\Omega_i = eB/(m_i c)$ is the ion gyrofrequency. The principal results of this paper are as follows:

1. The generation of ZFs in CTEM turbulence is studied analytically. The instability of ZFs is calculated from the quasi-neutrality condition, in which the ZF modulated

transport-induced radial current is balanced by the ZF potential shielded by the polarization effect, following the approach by Diamond et al.[24] The transport-induced radial current is related to the wave action density N whose evolution is described by the wave kinetic equation.[24,27,28]

2. An analytic expression for ZF growth rate in CTEM turbulence is derived by using the generalized polarization shielding for arbitrary radial wavelength.[29] This is an extension of the existing ZF generation theories[24,25] using the R-H polarization shielding which is based on a usual assumption of $q_r\rho_{\theta i} \ll 1$.

3. A relatively short spatial scale ZF, i.e., $q_r\rho_{\theta i} \sim 1$, is predicted to be generated by CTEM turbulence. For the parameters considered in this work, the normalized growth rate of ZFs increases with decreasing $k_\perp\rho_i$, τ, and increasing $\eta_e = L_n/L_{T_e}$ (decreasing R/L_n or increasing R/L_{T_e}). The regime of ZF radial scales corresponding to ZF growth becomes wider with decreasing τ, and increasing η_e, but changes very slightly with $k_\perp\rho_i$.

The remainder of this paper is organized as follows. In Sec. II, we present the analytic model employed in this work. In Sec. III, we give the principal results and discussion. Finally, we summarize our work, and discuss the limitations of the analytic model applied in this work, in Sec. IV.

II. ANALYTICAL MODEL

The turbulence-driven radial current is modulated by the ZF potential according to[24]

$$en_0\chi_z\tau\frac{\partial}{\partial t}\Phi_z = \frac{\partial}{\partial r}\left(\frac{\delta J_r}{\delta\phi_z}\Phi_z\right), \tag{1}$$

where χ_z denotes the generalized polarization shielding[29] of the ZF potential ϕ_z. Here, $\Phi_z = e\phi_z/T_e$ is the normalized ZF potential, and J_r is the turbulence-driven radial current. The radial current is related to the convective fluxes,[27] i.e.,

$$J_r = en_0(\langle\tilde{v}_r\hat{n}_i\rangle - \langle\tilde{v}_r\hat{n}_e\rangle), \tag{2}$$

where $\hat{n}_{i,e} = \tilde{n}_{i,e}/n_0$ are the normalized ion and electron density fluctuations, $\tilde{v}_r = -ik_\theta c_s \rho_s \Phi_k$, with $c_s = \sqrt{T_e/m_i}$, $\rho_s = c_s/\Omega_i$, and $\Phi_k = e\phi_k/T_e$ is the normalized potential fluctuation, and $\langle \cdots \rangle$ denotes a flux surface average. By using the relationships between the density and potential fluctuations for ions and electrons, the radial current is given by

$$J_r = -en_0 c_s \rho_s \sum_k k_\theta \gamma_k \left. \frac{\partial \chi}{\partial \omega} \right|_{\omega_k} |\Phi_k|^2 . \tag{3}$$

Here, γ_k is linear growth rate of the CTEM, and χ is the difference of the real parts of the ion and electron susceptibilities.

Furthermore, for drift waves propagating in a weakly inhomogeneous media with slowly varying parameters, we can define the wave action density $N(\mathbf{k}, \mathbf{r}, t)$ in $(\mathbf{k}, \mathbf{r})$ phase space[30] with the help of the energy conservation theorem,[27]

$$N_k = \frac{E_k}{\omega_k} = -\frac{n_0 T_e}{2} \left. \frac{\partial \chi}{\partial \omega} \right|_{\omega_k} |\Phi_k|^2 . \tag{4}$$

Here, the sign "$-$" is used to make sure $N_k > 0$, which is different from the definition of Ref. 27. It has the same form as a quantum number in a quantum mechanical system, and can be considered as an adiabatic invariant. Then we can relate the radial current and the wave action density N_k by substituting Eq. (4) into Eq. (3)

$$J_r = 2\frac{e c_s \rho_s}{T_e} \sum_k k_\theta \gamma_k N_k. \tag{5}$$

Now, we substitute Eq. (5) into Eq. (1), so that the ZF modulation of the turbulence-driven current in Eq. (1) is replaced by the ZF modulation of N_k. Thus, the frequency of the ZF, Ω_{ZF}, with radial wave number q_r, can be written as

$$\Omega_{ZF} = 2\frac{q_r}{\chi_z \tau} \frac{c_s \rho_s}{T_e} \sum_k k_\theta \gamma_k \frac{\delta N_k}{\delta \Phi_z}. \tag{6}$$

Evolution of the wave action density N_k is described by the wave kinetic equation[24,27,28]

$$\frac{\partial}{\partial t} N_k + (\mathbf{v}_g + \mathbf{v}_{ZF}) \cdot \frac{\partial N_k}{\partial \mathbf{r}} - \frac{\partial}{\partial \mathbf{r}} (\omega + \mathbf{k} \cdot \mathbf{v}_{ZF}) \cdot \frac{\partial N_k}{\partial \mathbf{k}} = \gamma_k N_k - \frac{\triangle \omega_k}{N_0} N_k^2, \tag{7}$$

where $\mathbf{v}_g$ is the drift wave group velocity, $\mathbf{v}_{ZF}$ is the ZF part of the $\mathbf{E} \times \mathbf{B}$ drift, and the second term on the RHS represents the nonlinear coupling. N_k can be separated into an equilibrium part $\langle N_k \rangle$ and a ZF modulated part $\tilde{N}_k$. $\tilde{N}_k$ is given by $\tilde{N}_k = (\delta N_k/\delta \Phi_z)\Phi_z$, which evolves on the ZF time scale Ω_{ZF} and the spatial scale $(q_r, 0, 0)$. The modulation part can be obtained by linearization of Eq. (7),[24]

$$\frac{\delta N_k}{\delta \Phi_z} = -iq_r^2 \frac{k_\theta c_s \rho_s}{\Omega_{ZF} - q_r v_{gr} + i\gamma_k} \left(1 - \frac{\chi_z}{\omega_{*e}/\omega_k}\right) \frac{\partial \langle N_k \rangle}{\partial k_r}, \tag{8}$$

where $\omega_{*e} = k_\theta c_s \rho_s / L_n$ is the electron diamagnetic frequency. Note that the modulated density gradient contribution alongside the equilibrium density gradient results in the second term (< 1) in the parentheses of last equation,[24,28] i.e.,

$$\begin{aligned} \frac{\partial \omega}{\partial r} &= \frac{1}{\omega_{*e}/\omega} k_\theta c_s \rho_s \frac{\partial}{\partial r} \left(\frac{1}{L_n} - \chi_z \frac{\partial}{\partial r} \Phi_z \right) \\ &= q_r^2 k_\theta c_s \rho_s \frac{1}{\omega_{*e}/\omega} \chi_z \Phi_z. \end{aligned} \tag{9}$$

Finally, substituting Eq. (8) into Eq. (6), we obtain the ZF growth rate

$$\gamma_{ZF} = \frac{2}{\chi_z \tau} q_r^4 c_s^2 \rho_s^2 \sum_k k_\theta^2 \frac{\gamma_k v_{gr}}{(\Omega_{ZF} - q_r v_{gr})^2 + \gamma_k^2} \left(1 - \frac{\chi_z}{\omega_{*e}/\omega_k}\right) \frac{\partial \langle N_k \rangle / \partial k_r}{n_0 T_e}. \tag{10}$$

In Eq. (10), $v_{gr} < 0$, and the term in parentheses is positive, so we expect growth, $\gamma_{ZF} > 0$, for $\partial \langle N_k \rangle / \partial k_r < 0$, i.e., for a monotonically decaying spectrum.[1,24] The ZF growth rate given by Eq. (10) is the generalization of Eq. (6a) in Ref. 24. We can recover the result of Ref. 24 by taking the susceptibility as $\chi = \omega_{*e}/\omega - k_\perp^2 \rho_s^2 - 1$ and R-H formula of neoclassical polarization shielding $\chi_z = 1.6\tau\epsilon^{3/2} q_r^2 \rho_{\theta i}^2$, respectively.

In this work, the susceptibility and linear growth rate of the CTEM are taken from Ref. 5 where only resonant trapped electron drive is considered. In reality, nonresonant trapped electrons' contributions can be nonnegligible.

$$\begin{aligned} \chi &= -[1 - \sqrt{2\epsilon} + \tau(1 - \Gamma_0)] + \frac{\omega_{*e}}{\omega} \left[\Gamma_0 + \eta_i b_i (\Gamma_1 - \Gamma_0) - \sqrt{2\epsilon} \left(1 - 1.5G \frac{L_n}{R} \right) \right] \\ &= A + B \frac{\omega_{*e}}{\omega}, \end{aligned} \tag{11}$$

$$\gamma_k = 2\sqrt{2\pi\epsilon}\, \eta_e \left(\frac{R}{L_n G} \right)^{3/2} \left(\frac{R}{L_n G} - \frac{3}{2} \right) \exp\left(-\frac{R}{L_n G} \right). \tag{12}$$

Here, $A = -[1 - \sqrt{2\epsilon} + \tau(1 - \Gamma_0)]$, $B = \left[\Gamma_0 + \eta_i b_i(\Gamma_1 - \Gamma_0) - \sqrt{2\epsilon}\,(1 - 1.5GL_n/R)\right]$, and γ_k is normalized by ω_{*e}. $\eta_i = L_n / L_{T_i}$, where $L_{T_i}^{-1} \equiv -\partial \ln T_i / \partial r$ is the normalized ion temperature gradient. $\Gamma_n = I_n(b_i)\exp(-b_i)$ with I_n a modified Bessel function, $b_i = k_\perp^2 \rho_i^2$. G is a function of magnetic shear $\hat{s}$ and azimuthal angle θ_0 of the turning point of a trapped electron. The geometry considered has circular, concentric magnetic surfaces with large aspect ratio. We use the explicit expression $G = 0.64\hat{s} + 0.57$ which is obtained by averaging over θ_0.[31,32] For simplicity, we take a monochromatic wave packet, i.e., $\langle N_k \rangle = N_0 \delta(\mathbf{k} - \mathbf{k}_0)$ with $\mathbf{k_0} = (k_{r0},\, k_{\theta 0})$.[33] We approximate the summation in $\mathbf{k}$ in Eq. (10) by an integration. After an integration by parts, then we can obtain the final analytic formula for the ZF growth rate

$$\gamma_{ZF} = \frac{1}{\chi_z \tau} q_r^4 c_s^2 \rho_s^2 k_{\theta 0}^2 \left.\frac{\partial \chi}{\partial \omega}\right|_{\omega_{k_0}} \left.\frac{\partial}{\partial k_r}\left[\frac{\gamma_k v_{gr}}{q_r^2 v_{gr}^2 + \gamma_k^2}\left(1 - \frac{\chi_z}{\omega_{*e}/\omega_k}\right)\right]\right|_{k_0} |\Phi_{k_0}|^2 , \tag{13}$$

where the assumption $\gamma_{ZF} \ll \gamma_k$ is used.

We use the generalized expression for polarization shielding for arbitrary radial wavelength in Ref. 29,

$$\begin{aligned}\chi_z \;=\; & 1 - \Gamma_0(q_r^2\rho_i^2) + \left\{ \frac{1}{1.83\epsilon^{3/2} q_r^2 \rho_{\theta i}^2} + \left[1 + \frac{\sqrt{8\epsilon}}{\pi}\Gamma'_{tr} + \left(1 - \frac{\sqrt{8\epsilon}}{\pi}\right)\Gamma'_p\right] \frac{1}{1 + q_r^2\rho_i^2} \right. \\ & \left. + \sqrt{\frac{\pi^3}{2}} q_r \rho_i \left[1 + \frac{\sqrt{8\epsilon}}{\pi}\Gamma_{tr} + \left(1 - \frac{\sqrt{8\epsilon}}{\pi}\right)\Gamma_p\right] \frac{q_r^2\rho_i^2}{1 + q_r^2\rho_i^2} \right\}^{-1} ,\end{aligned} \tag{14}$$

with $\Gamma_{tr} = 0.916/(\sqrt{\pi\epsilon} q_r \rho_{\theta i})$, $\Gamma_p = 1/(2\sqrt{2\pi}\epsilon q_r \rho_{\theta i})$, $\Gamma'_{tr} = 2\Gamma_{tr}/\pi$, and $\Gamma'_p = 2\Gamma_p/\pi$. The details of the calculation can be found in Ref. 29. Here, we explain the physical meaning of each term in Eq. (14). $1 - \Gamma_0$ is the well known classical polarization shielding, and the remaining terms are the contributions to the neoclassical part which is constructed by adding the inverse of the asymptotic forms in the limiting cases and then taking the inverse of the summation. The first term in the large bracket is the inverse of the results in the long wavelength limit which has the same scaling as the R-H formula with a slightly different coefficient. $\sqrt{8\epsilon}/\pi$ is the fraction of trapped particles, and $1 - \sqrt{8\epsilon}/\pi$ is the passing particle fraction. $\Gamma_{tr}(\Gamma'_{tr})$ and $\Gamma_p(\Gamma'_p)$ are the contributions from trapped particles and passing particles, respectively, in the short (intermediate) wavelength limit, where $\Gamma_{tr}(\Gamma'_{tr})$ and $\Gamma_p(\Gamma'_p)$ are inversely proportional to the banana width $\sqrt{\epsilon}\rho_{\theta i}$, and the radial deviation from the flux surface for a strongly circulating particle $\epsilon\rho_{\theta i}$, respectively. The factor $\sqrt{\pi^3} q_r \rho_i/\sqrt{2}$ is the inverse of the FLR effects in the short wavelength limit. This addition of terms in the denominator may produce a smaller value of the neoclassical polarization in an intermediate region. To partially compensate for the artifact of the connection formula in the intermediate region, the factors $1/(1+q_r^2\rho_i^2)$ and $q_r^2\rho_i^2/(1+q_r^2\rho_i^2)$ are multiplied by the inverse of the results in the short and intermediate wavelength limits, respectively. They are slightly less than 1 in their validity regimes respectively, with their sum equal to 1.

From this point, the second term in the parentheses of Eq. (13) is ignored for simplicity. Therefore, the normalized ZF growth rate can be expressed explicitly as

$$\frac{\gamma_{ZF}}{\frac{v_{Ti}}{R}(\frac{R}{\rho_i})^2\left|\frac{e\phi_{k_0}}{T_i}\right|^2} = \frac{\triangle^2 B}{\tau^2 R/L_n}\gamma_{k_0}V_{gr}\left[1+2k_{r0}^2\rho_i^2\left(\frac{\triangle''}{\triangle'}-\frac{2\triangle'}{\triangle}\right)\right] \frac{q_r^4\rho_{\theta i}^4\epsilon^4/q^4}{\chi_z}\frac{V_{gr}^2 q_r^2\rho_{\theta i}^2\epsilon^2/q^2-\gamma_{k_0}^2}{(V_{gr}^2 q_r^2\rho_{\theta i}^2\epsilon^2/q^2+\gamma_{k_0}^2)^2}. \quad (15)$$

Here, the ZF growth rate is normalized by $(V_{Ti}/R)(R/\rho_i)^2|e\phi_{k_0}/T_i|^2$, where $V_{Ti}=\sqrt{T_i/m_i}$, so that all the temperature ratio and density gradient dependencies are included on the RHS of Eq. (15) for given T_i. q is the safety factor. V_{gr} is normalized with respect to $\rho_i\omega_{*e}$, i.e., $V_{gr}=-2k_{r0}\rho_i\triangle'/\triangle^2$ with $\triangle=-A/B$. "$\prime$" denotes the derivative with respect to b_i, and $k_{r0}=k_{\theta 0}$ is used in the following. In the last equation, $V_{gr}<0$, so the regime of the ZF radial scale for ZF growth is $0<q_r\rho_{\theta i}<\gamma_{k_0}/(|V_{gr}|\,\epsilon/q)$.

III. PARAMETRIC DEPENDENCIES OF ANALYTIC RESULTS

We have presented the analytic expression for the ZF growth rate in the last section. Now, we investigate its parametric dependence. We choose the following basic parameters: $q=1.4$, $\hat{s}=0.8$, $\epsilon=0.18$, $R/L_{Ti}=0$, $R/L_{Te}=6.9$, $R/L_n=2.2$, and $\tau=1$. First, the normalized ZF growth rate as a function of ZF wavelength $q_r\rho_{\theta i}$ is displayed in Fig. 1, with the wavelength of the CTEM as a parameter and the other parameters fixed. From this figure, we can see that the radial scale of the ZF corresponding to the maximum growth rate satisfies $q_r\rho_{\theta i}\sim 1$. The normalized ZF growth rate increases with increasing wavelength of the ambient CTEM, whereas the regime of the ZF radial scale corresponding to ZF growth changes very slightly.

Next, in Fig. 2, the normalized ZF growth rate as a function of $q_r\rho_{\theta i}$ is displayed, with τ as a parameter and the other parameters fixed. The normalized ZF growth rate decreases and the regime of the ZF radial scale corresponding to ZF growth becomes narrower with increasing τ. This trend for the normalized ZF growth rate can be seen explicitly from Eq. (15). The normalized linear growth rate of CTEM is independent on τ in this model.

$|V_{gr}|$ increases with increasing τ, if one analyzes the expression for V_{gr} carefully. These two factors result in the narrower regime of the ZF radial scale corresponding to the higher τ, although the latter can not be seen easily. A weak ZF effect on the transport level for large τ was reported in gyrokinetic simulations of CTEM turbulence.[16,19]

Finally, the normalized ZF growth rates as a function of $q_r\rho_{\theta i}$ are displayed in Fig. 3 and Fig. 4, with R/L_n and R/L_{T_e} as parameters, respectively. For this case, $R/L_{Ti} = 2.2$ is fixed to be the same as in Ref. 21, and the other parameters are fixed to be the same as above. The normalized ZF growth rate increases and the regime of the ZF radial scale corresponding to ZF growth becomes wider with increasing η_e (decreasing R/L_n or increasing R/L_{T_e}). We can understand this from Eq. (12) and Eq. (15). The normalized linear growth rate of the CTEM γ_k, i.e., Eq. (12), increases with increasing η_e. On the other hand, there is a factor of $1/(R/L_n)$ in the normalized ZF growth rate, Eq. (15). These result in an increase of the normalized ZF growth rate as η_e increases. $V_{gr}\epsilon/q$ is weakly dependent of R/L_n, and independent on R/L_{T_e}. Therefore, from the analysis of Eq. (15) in the last section, the regime of the ZF radial scale corresponding to ZF growth is wider for larger η_e. The analytic expression for the growth rate of the ZF obtained in Ref. 23 also increases with η_e below the resonant point. However, the resonant behavior in Ref. 23 comes from the advanced fluid closure[34] for the relation between potential fluctuations and electron temperature fluctuations which is not used in our analytic derivation. Such resonant behavior of ZF growth still remains to be observed in gyrokinetic simulations. An important role of ZFs in regulating TEM turbulence was found in recent simulations[21] for $R/L_{T_i} = 2.2$, $R/L_n = 2.2$, $R/L_{T_e} = 6.9$, and $\tau = 1$ where strong normalized ZF growth is predicted by our analytic formula.

IV. CONCLUSIONS

In the present work, we investigated the ZF generation in CTEM turbulence. The quasi-neutrality condition is used, in which the ZF potential shielded by polarization effects balances the ZF modulated transport-induced radial current.[24] The evolution of the wave action density N is described by the wave kinetic equation.[24,27,28] For simplicity, we adopt the theory of Ref. 5 for the susceptibility and the linear growth rate of the CTEM. Based on the theoretical assumptions above, we derive an analytic expression for the ZF growth rate in CTEM turbulence in which the generalized polarization shielding for arbitrary radial wavelengths is used.[29] It extends the existing ZF generation theories[24,25] using the R-H polarization shielding, which is valid for the long wavelength limit, i.e., $q_r \rho_{\theta i} \ll 1$, to a wider regime of ZF radial scales.

We obtain a fine-scale ZF with $q_r \rho_{\theta i} \sim 1$ generated by CTEM turbulence for the parameter regime considered in this work. The validity regime has been extended by employing a generalized polarization shielding which can be used for arbitrary wavelength[29] rather than the R-H formula for the long wavelength limit. We also investigate the variation of the ZF growth rate with plasma parameters. The normalized ZF growth rate increases with increasing wavelength of the ambient CTEM, decreasing τ, and increasing η_e. The stronger ZF growth with higher η_e is qualitatively consistent with previous analytic theory[23] when η_e is below the resonant point in Ref. 23. We obtain small normalized ZF growth rates for high τ where the ZF influence on the transport level is weak,[16,19] and strong normalized ZF growth rates for $R/L_{T_i} = 2.2$, $R/L_n = 2.2$, $R/L_{T_e} = 6.9$, and $\tau = 1$ where the ZF effects are important,[21] respectively. The regime of ZF radial scales corresponding to ZF growth becomes wider with decreasing τ and increasing η_e, but changes very slightly with the wave number of the ambient CTEM.

Finally, we discuss limitations of the analytic model adopted in this work. We used a simple model for linear growth of the CTEM[5] which does not include the nonresonant trapped particles. The zonal density which possibly plays a dominant role in saturating the TEM turbulence in some parameter regimes[19,35] is not studied explicitly in this work. In addition, there's no guarantee that the eikonal description of the wave kinetic approach will work well for the fine-scale ZF generation driven by CTEM turbulence. We have used the wave kinetic equation for the wave action density in our derivation because the efficiency of this approach, which relies mostly on conservation laws rather than on a particular nonlinear mode coupling channel involving a few modes, has been demonstrated before.[24] However, we have to assume a spatial scale separation between the ambient CTEM turbulence and the ZFs when we linearize the wave kinetic equation. There exists the same limitation in Ref. 23. In Ref. 36, it was reported that the assumption of spatial scale separation between the background ITG turbulence the and the ZFs does not affect the results much, by comparing the results from the wave kinetic approach and those from the coherent mode coupling[25] method. Possible artifacts which originate from assuming the spatial scale separation between the ambient CTEM turbulence and the ZFs have not been checked yet. In the future, we will employ the coherent mode coupling method for ZF generation in CTEM turbulence and compare the results of these two methods.

Recently, new insight has been gained on the ZF dynamics by considering the inviscid invariance of the potential vorticity.[37] The resulting momentum theorem states that in the absence of turbulent transport, dissipation and turbulence spreading, stationary turbulence cannot excite a ZF. In most analytic theories of ZF generation, the growth of turbulence (i.e., nonstationarity) plays a crucial role. Extending the aforementioned momentum theorem to turbulence models such as ITG and CTEM which are more directly relevant to tokamak confinement physics should be rewarding. Finally, the drift-wave-ZF system behavior cannot be completely understood without considering the random shearing[22,24] of drift wave turbulence via ZFs.

Acknowledgments

We thank Y. Xiao, L. Chen, P. H. Diamond, Z. Lin, J. Lang, D. Ernst, G. Rewoldt, and G. Dif-Pradalier for useful comments on our work. This work was supported by the China Scholarship Council (LW), U. S. Department of Energy Contract No. DE–AC02–09CH11466 (TSH, LW), the U. S. DOE SciDAC center for Gyrokinetic Particle Simulation of Turbulent Transport in Burning Plasmas, and the U. S. DOE SciDAC-FSP Center for Plasma Edge Simulation (TSH).

1 P. H. Diamond, S.-I. Itoh, K. Itoh, and T. S. Hahm, Plasma Phys. Control. Fusion **47**, R35 (2005).

2 A. Fujisawa, Nucl. Fusion **49**, 013001 (2009).

3 Z. Lin, T. S. Hahm, W. W. Lee, W. M. Tang, and R. B. White, Science **281**, 1835 (1998).

4 A. M. Dimits, G. Bateman, M. A. Beer, et al., Phys. Plasmas **7**, 969 (2000).

5 J. C. Adam, W. M. Tang, and P. H. Rutherford, Phys. Fluids **19**, 561 (1976).

[6] L. Chen, R. L. Berger, J. G. Lominadze, M. N. Rosenbluth, and P. H. Rutherford, Phys. Rev. Lett. **39**, 754 (1977).

[7] P. H. Diamond, P. L. Similon, P. W. Terry, C. W. Horton, S. M. Mahajan, J. D. Meiss, M. N. Rosenbluth, K. Swartz, T. Tajima, R.D. Hazeltine, D. W. Ross, 10th IAEA Fusion Energy Conference, Baltimore, USA, 1982 (International Atomic Energy Agency, Vienna, 1982), paper No. IAEA-CN-41/D-1-2.

[8] F. Y. Gang and P. H. Diamond, Phys. Fluids B **2**, 2976 (1990).

[9] F. Y. Gang, P. H. Diamond, and M. N. Rosenbluth, Phys. Fluids B **3**, 68 (1991).

[10] T. S. Hahm and W. M. Tang, Phys. Fluids B **3**, 989 (1991).

[11] T. S. Hahm, Phys. Fluids B **3**, 1445 (1991).

[12] M. A. Beer and G. W. Hammett, Phys. Plasmas, **3**, 4018 (1996).

[13] F. Ryter, F. Imbeaux, F. Leuterer, H.-U. Fahrbach, W. Suttrop, and ASDEX Upgrade Team, Phys. Rev. Lett. **86**, 5498 (2001).

[14] D. R. Ernst, P. T. Bonoli, P. J. Catto, W. Dorland, C. L. Fiore, R. S. Granetz, M. Greenwald, A. E. Hubbard, M. Porkolab, M. H. Redi, J. E. Rice, and K. Zhurovich, Phys. Plasmas **11**, 2637 (2004).

[15] J. C. DeBoo, S. Cirant, T. C. Luce, A. Manini, C. C. Petty, F. Ryter, M. E. Austin, D. R. Baker, K. W. Gentle, C. M. Greenfield, J. E. Kinsey, and G. M. Staebler, Nucl. Fusion **45**, 494 (2005).

[16] T. Dannert and F. Jenko, Phys. Plasmas **12**, 072309 (2005).

[17] Z. Lin, L. Chen, I. Holod, Y. Nishimura, H. Qu, S. Ethier, G. Rewoldt, W. X. Wang, Y. Chen, J. Kohut, S. Parker, and S. Klasky, in Proceedings of the 21st International Conference on Plasma Physics and Controlled Nuclear Fusion Research, Chengdu, China, 2006 (International Atomic Energy Agency, Vienna, 2006), paper No. IAEA-CN-138/TH/P2-8.

[18] J. Lang, Y. Chen, and S. E. Parker, Phys. Plasmas **14**, 082315 (2007).

[19] J. Lang, S. E. Parker, and Yang Chen, Phys. Plasmas **15**, 055907 (2008).

[20] D. R. Ernst, J. Lang, W. M. Nevins, M. Horrman, Y. Chen, W. Dorland, and S. Parker, Phys. Plasmas **16**, 055906 (2009).

[21] Y. Xiao and Z. Lin, "Turbulent transport of trapped electron modes in collisionless plasmas", submitted to Phys. Rev. Lett. (2009).

[22] T. S. Hahm, M. A. Beer, Z. Lin, G. W. Hammett, W. W. Lee, and W. M. Tang, Phys. Plasmas **9**, 922 (1999).

[23] J. Anderson, H. Nordman, R. Singh, and J. Weiland, Plasma Phys. Control. Fusion **48**, 651 (2006).

[24] P. H. Diamond, M. N. Rosenbluth, F. L. Hinton, et al., in Plasma Physics and Controlled Nuclear Fusion Research, 18th IAEA Fussion Energy Conference, Yokohama, Japan, 1998 (International Atomic Energy Agency, Vienna, 1998), paper No. IAEA-CN-69/TH3/1.

[25] L. Chen, Z. Lin, and R. White, Phys. Plasmas **7**, 3129 (2000).

[26] M. N. Rosenbluth, F. L. Hinton, Phys. Rev. Lett. **80**, 724 (1998).

[27] P. H. Diamond and Y.-B. Kim, Phys. Fluids B **3**, 1626 (1991).

[28] M. A. Malkov and P. H. Diamond, Phys. Plasmas **8**, 3996 (2001).

[29] Lu Wang and T. S. Hahm, "Generalized expression for polarization density", to appear in Phys. Plasmas (2009).

[30] V. B. Lebedev, P. H. Diamond, et al., Phys. Plasmas **2**, 4420 (1995).

[31] W. M. Tang, Theory of Fusion Plasmas, ed. J. Vaclavik, F. Troyon, and E. Sindoni (Bologna: Editrice Compositori) p. 31 (1990).

[32] J. Li and Y. Kishimoto, Plasma Phys. Controlled Fusion **44**, A479 (2002).

[33] A. I. Smolyakov, P. H. Diamond, and V. I. Shevchenko, Phys. Plasmas **7**, 1349 (2000).

[34] J. Weiland, Collective Modes in Inhomogeneous Plasmas, Kinetic and Advanced Fluid Theory (Bristol: Institute of Physics Publishing) p. 115 (2000).

[35] R. Gatto and P. W. Terry, Phys. Plasmas **13**, 022306 (2006).

[36] J. Anderson and Y. Kishimoto, Phys. Plasmas **14**, 012308 (2007).

[37] P. H. Diamond, O. D. Gurcan, T. S. Hahm, K. Miki, Y. Kosuga, and X. Garbet, Plasma Phys. Controlled Fusion **50**, 124018 (2008).

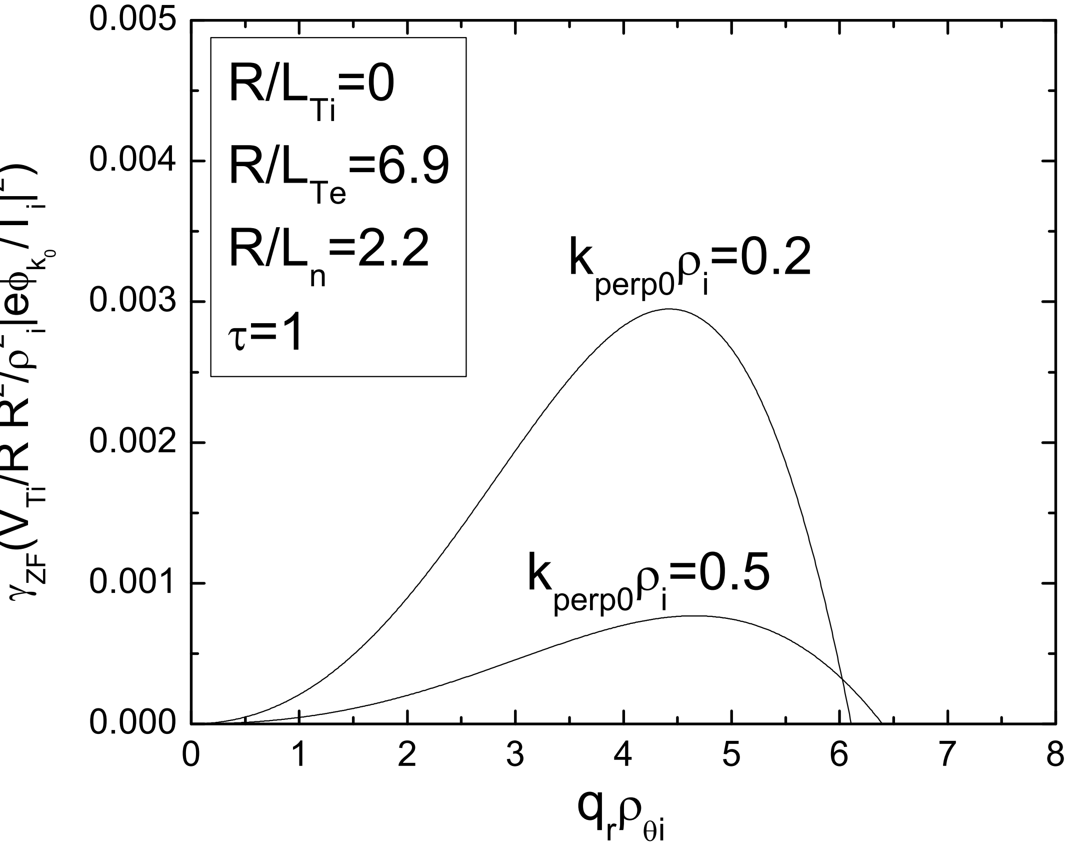

FIG. 1: Normalized ZF growth rate versus ZF wavelength $q_r\rho_{\theta i}$ with the wavelength of the ambient CTEM, $k_{\perp 0}\rho_i$, as a parameter.

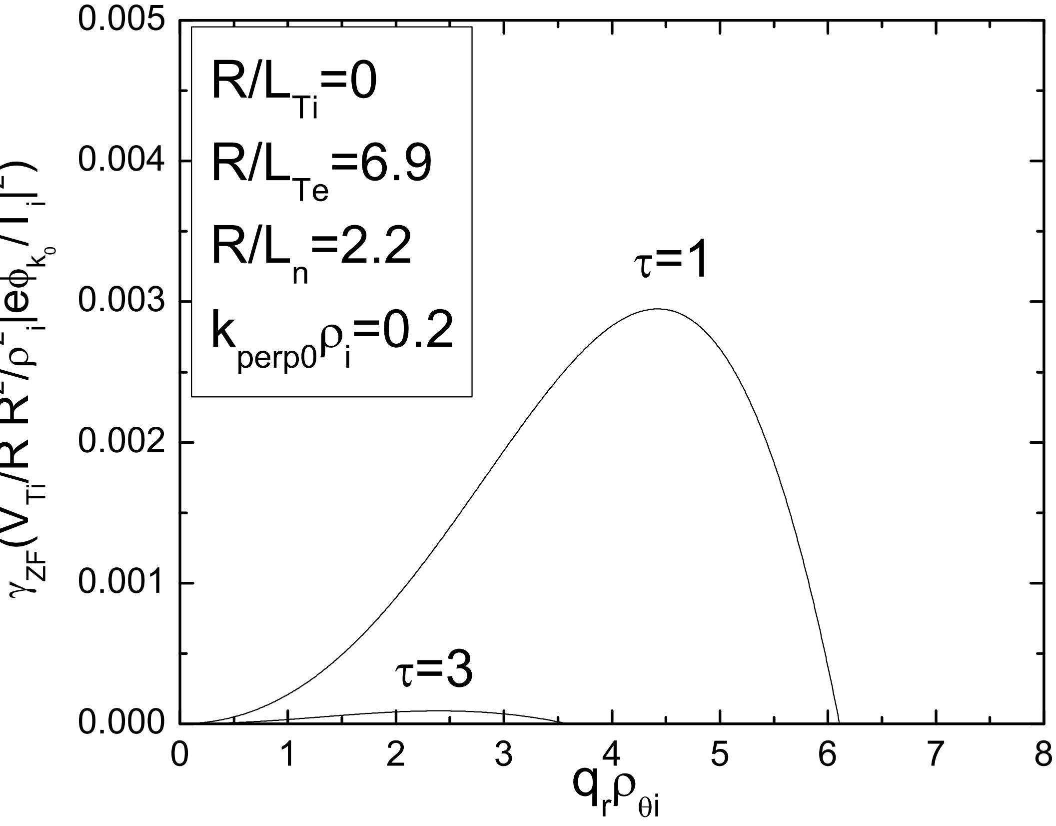

FIG. 2: Normalized ZF growth rate versus ZF wavelength $q_r\rho_{\theta i}$ with τ as a parameter.

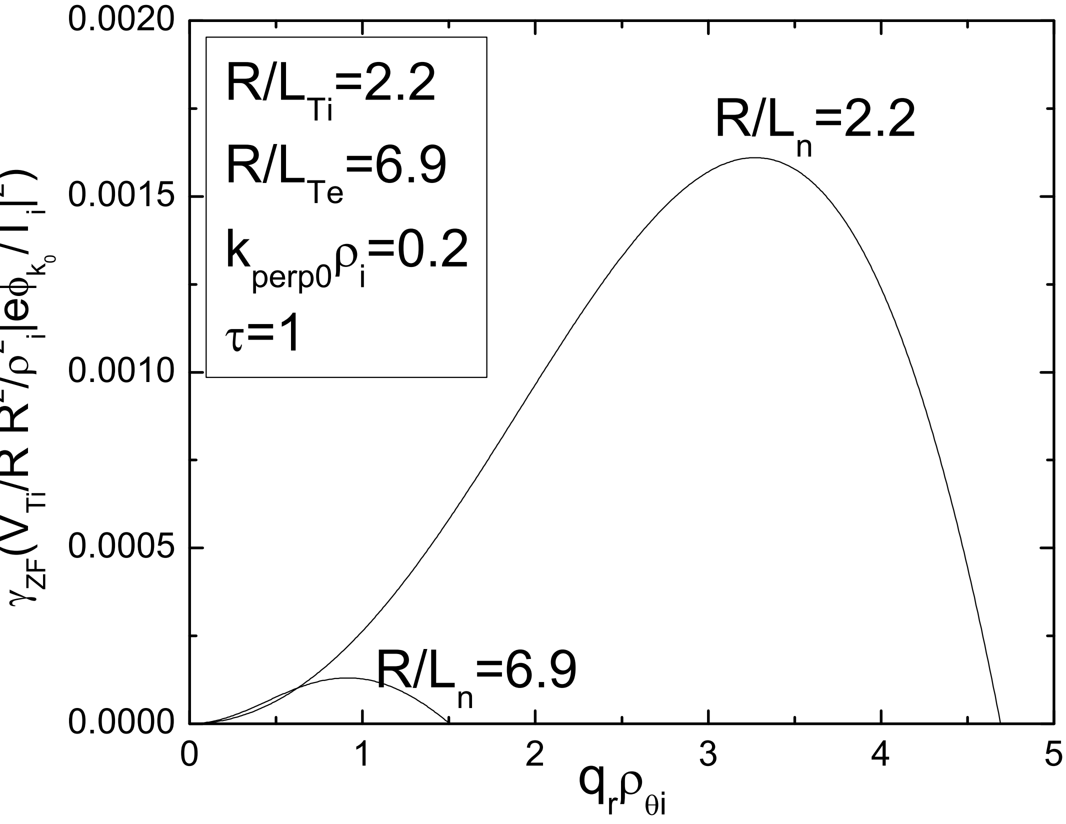

FIG. 3: Normalized ZF growth rate versus ZF wavelength $q_r\rho_{\theta i}$ with R/L_n as a parameter.

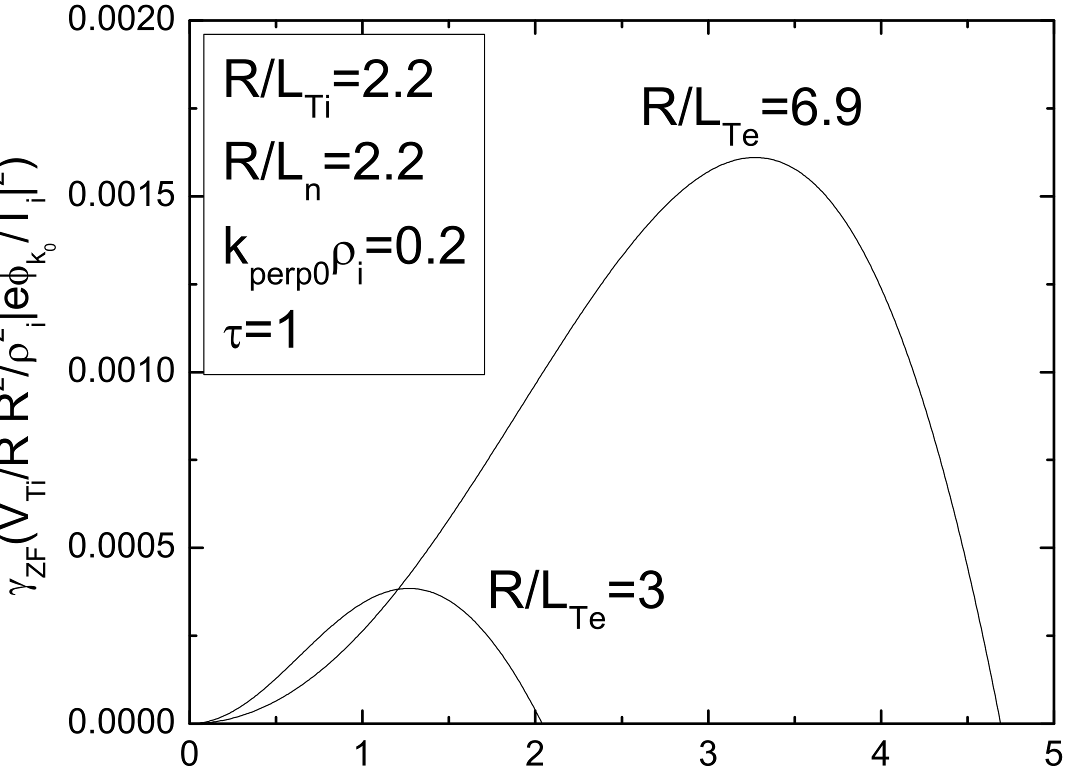

FIG. 4: Normalized ZF growth rate versus ZF wavelength $q_r\rho_{\theta i}$ with R/L_{T_e} as a parameter.

The Princeton Plasma Physics Laboratory is operated
by Princeton University under contract
with the U.S. Department of Energy.

Information Services
Princeton Plasma Physics Laboratory
P.O. Box 451
Princeton, NJ 08543

Phone: 609-243-2750
Fax: 609-243-2751
e-mail: pppl_info@pppl.gov
Internet Address: http://www.pppl.gov